Journal of Steroid Biochemistry and Molecular Biology 212 (2021) 105945

Contents lists available at ScienceDirect

Journal of Steroid Biochemistry and Molecular Biology

journal homepage: www.elsevier.com/locate/jsbmb

Crystal structure of an apo 7α-hydroxysteroid dehydrogenase reveals key structural changes induced by substrate and co-factor binding

Ki-Hwa Kim [a], Chang Woo Lee [b], Bashu Dev Pardhe [a], Jisub Hwang [b,c], Hackwon Do [b], Yung Mi Lee [d], Jun Hyuck Lee [b,c,*], Tae-Jin Oh [a,e,f,**]

[a] Department of Life Science and Biochemical Engineering, Graduate School, SunMoon University, Asan, 31460, Republic of Korea
[b] Research Unit of Cryogenic Novel Material, Korea Polar Research Institute, Incheon, 21990, Republic of Korea
[c] Department of Polar Sciences, University of Science and Technology, Incheon, 21990, Republic of Korea
[d] Division of Life Sciences, Korea Polar Research Institute, Incheon, 21990, Republic of Korea
[e] Genome-based BioIT Convergence Institute, Asan, 31460, Republic of Korea
[f] Department of Pharmaceutical Engineering and Biotechnology, SunMoon University, Asan, 31460, Republic of Korea

ARTICLE INFO

Keywords:
Crystal structure
Conformational change
7α-hydroxysteroid dehydrogenase
X-ray crystallography

ABSTRACT

7α-Hydroxysteroid dehydrogenase (7α-HSDH) catalyzes the dehydrogenation of a hydroxyl group at the 7α position in steroid substrates using NAD^+ or $NADP^+$ as a co-factor. Although studies have determined the binary and ternary complex structures, detailed structural changes induced by ligand and co-factor binding remain unclear, because ligand-free structures are not yet available. Here, we present the crystal structure of apo 7α-HSDH from *Escherichia coli* (*Eco*-7α-HSDH) at 2.7 Å resolution. We found that the apo form undergoes substantial conformational changes in the β4-α4 loop, α7-α8 helices, and C-terminus loop among the four subunits comprising the tetramer. Furthermore, a comparison of the apo structure with the binary (NAD^+)-complex and ternary (NADH and 7-oxoglycochenodeoxycholic acid)-complex *Eco*-7α-HSDH structures revealed that only the ternary-complex structure has a fully closed conformation, whereas the binary-complex and apo structures have a semi-closed or open conformation. This open-to-closed transition forces several catalytically important residues (S146, Y159, and K163) into correct positions for catalysis. To confirm the catalytic activity, we used alcohol dehydrogenase for NAD^+ regeneration to allow efficient conversion of chenodeoxycholic acid to 7-ketolithocholic acid by *Eco*-7α-HSDH. These findings demonstrate that apo *Eco*-7α-HSDH exhibits intrinsically flexible characteristics with an open conformation. This structural information provides novel insight into the 7α-HSDH reaction mechanism.

1. Introduction

Intestinal bacteria can transform bile acids (steroid molecules) into secondary bile acids through enzymatic processes that mediate deconjugation, dehydroxylation, or dehydrogenation reactions [1]. Among them, microbial stereospecific dehydrogenation of steroid molecules in both α and β orientations have been reported [2]. In particular, 7α-hydroxysteroid dehydrogenase (7α-HSDH) is of great interest as a biocatalyst for the transformation of commercially useful steroid molecules [2,3]. For example, 7α-HSDH can be used for the bioconversion of chenodeoxycholic acid (CDCA) into ursodeoxycholic acid (UDCA), which helps reduce the cholesterol saturation of bile, thereby resulting in its application as a medical therapy for gallstone disease [4].

7α-HSDH reversibly catalyzes the oxidation of the C7 hydroxyl group of steroids using NAD^+ or $NADP^+$ as a co-factor. Several microbial 7α-HSDH enzymes have been identified and characterized in *Escherichia coli* [5–7], *Bacteroides fragilis* [8,9], *Xanthomonas maltophilia* [10], *Clostridium sordellii* [11], *Clostridium difficile* [12], and *Clostridium absonum* [13–15]. In recent years, many strategies have been developed for UDCA from CDCA synthesis using 7α-HSDH and 7β-HSDH. Each 7α-HSDH

Abbreviations: 7-KLCA, 7-ketolithocholic acid; ADH, alcohol dehydrogenase; *Bme*-7α-HSDH, *Brucella melitensis*-7α-hydroxysteroid dehydrogenase; *Cab*-7α-HSDH, *Clostridium absonum* 7α-hydroxysteroid dehydrogenase; CDCA, chenodeoxycholic acid; *Eco*-7α-HSDH, *Escherichia coli* 7α-hydroxysteroid dehydrogenase; *Eco*-ADH, *Escherichia coli* alcohol dehydrogenase; LC, liquid chromatography; MS, mass spectrometry; PDB, Protein Data Bank; UDCA, ursodeoxycholic acid.

* Corresponding author at: Research Unit of Cryogenic Novel Material, Korea Polar Research Institute, Incheon, 21990, Republic of Korea.
** Corresponding author at: Department of Pharmaceutical Engineering and Biotechnology, SunMoon University, Asan, 31460, Republic of Korea.
E-mail addresses: junhyucklee@kopri.re.kr (J.H. Lee), tjoh3782@sunmoon.ac.kr (T.-J. Oh).

https://doi.org/10.1016/j.jsbmb.2021.105945
Received 21 April 2021; Received in revised form 18 June 2021; Accepted 20 June 2021
Available online 23 June 2021
0960-0760/© 2021 Elsevier Ltd. All rights reserved.

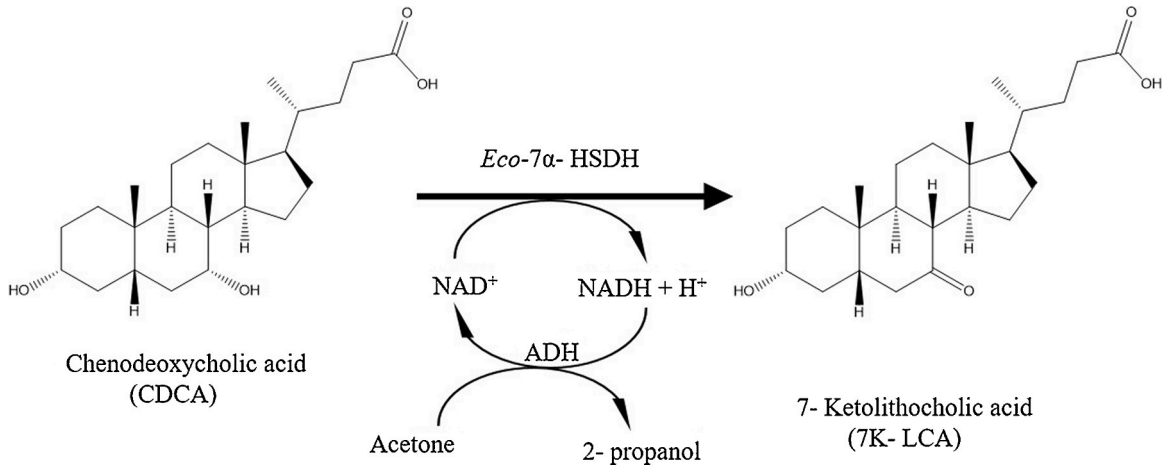

Scheme 1. Reaction catalyzed by *Eco*-7α-HSDH using the *Eco*-ADH system for NAD^+ regeneration.

Table 1
X-Ray diffraction data collection and refinement statistics.

Dataset	*Eco*-7α-HSDH
X-ray source	BL-5C beam line
Space group	$P2_1$
Unit-cell parameters (Å, °)	a = 58.8, b = 100.2, c = 160.2, α=γ = 90.00, β = 95.6
Wavelength (Å)	0.9794
Resolution (Å)	50.0–2.70 (2.75–2.70)
Total reflections	178,734
Unique reflections	50,045 (2487)
Average I/σ (I)	16.7 (2.7)
R_{meas} [a]	0.167 (0.756)
CC1/2	0.987 (0.776)
Redundancy	3.6 (3.8)
Completeness (%)	98.7 (100.0)
Refinement	
Resolution range (Å)	38.06–2.70 (2.75–2.70)
No. reflections in the working set	49,978 (2483)
No. reflections in the test set	2490 (124)
No. amino acid residues	1977
No. water molecules	126
Molecules per asymmetric unit	8
R_{cryst} [b]	0.195 (0.266)
R_{free} [c]	0.276 (0.369)
R.m.s. bond length (Å)	0.010
R.m.s. bond angle (°)	1.328
Average B-value (Å^2) (protein)	60.4
Average B-value (Å^2) (solvent)	49.1

Values in parentheses refer to the highest resolution shells.
R.m.s., root mean square.
[a] $R_{meas} = \sum_{hkl} \{N (hkl) / [N (hkl) - 1]\}^{1/2} \sum_i |I_i(hkl) - <I(hkl)>| / \sum_{hkl} \sum_i I (hkl)$.
[b] $R_{cryst} = \sum | |Fo| - |Fc| | / \sum |Fo|$.
[c] R_{free} was calculated using 5% of all reflections excluded from the refinement stages and using high-resolution data.

enzyme has a different co-factor preference and requires expensive nicotinamide co-factors [NAD(P)(H)] for substrate catalysis [16]. Moreover, utilization of well-established enzymatic strategies for the regeneration of nicotinamide co-factors can be applied to the synthesis of UDCA [17]. 7α-HSDH from *E. coli* (*Eco*-7α-HSDH) utilizes NAD^+, whereas 7α-HSDH from *C. absonum* (*Cab*-7α-HSDH) prefers $NADP^+$ as a co-factor. Additionally, *Cab*-7α-HSDH possesses positively charged residues (R16, R38, and R194) that interact specifically with the adenosine ribose C2 phosphate group of NADP.

To date, the crystal structures of *Eco*-7α-HSDHs [5], *Cab*-7α-HSDHs [14], and 7α-HSDH from *Brucella melitensis* [*Bme*-7α-HSDH; Protein Data Bank (PDB): 3GAF; not yet published] have been determined. These include two crystal structures of *Eco*-7α-HSDH in a binary complex with NAD (PDB: 1AHH) and a ternary complex with NADH and 7-oxoglycochenodeoxycholic acid (PDB: 1AHI) [5], and a crystal structure of *Cab*-7α-HSDH (PDB: 5EPO) in complex with taurochenodeoxycholic acid [tauro-(CDCA)] and NADP(+), which explained the NADP preference as a co-factor [14]. Notably, the crystal structure of apo *Bme*-7α-HSDH has also been determined (PDB: 3GAF), but related studies have not yet been published.

In this study, we present the first apo *Eco*-7α-HSDH structure at 2.7 Å resolution. Although the molecular details of the *Eco*-7α-HSDH protein have been previously reported in binary- and ternary-complex forms, the apo structure provides insight into novel conformational changes induced by substrate and co-factor recognition. Moreover, comparative structural analysis with previously determined structures shows that the β4-α4 loop, α7-α8 helices, and C-terminal loop are important elements for co-factor and substrate binding. Furthermore, we demonstrated the use of an NAD^+-regeneration system using *Eco*-alcohol dehydrogenase (ADH) for CDCA biotransformation by *Eco*-7α-HSDH. These findings offer new insight into the mechanism of *Eco*-7α-HSDH activity.

2. Materials and methods

2.1. Chemicals and materials

CDCA, 7-ketolithocholic acid (7-KLCA), acetone, kanamycin, and NAD^+ were purchased from Sigma-Aldrich (Seoul, Korea). Commercial ADH-2 protein was purchased from Cambrex (Wiesbaden, Germany).

2.2. Cloning and protein purification

The gene encoding *Eco*-7α-HSDH (UniProtKB: P0AET8) and that encoding ADH (UniProtKB: P37686) from *E. coli* (*Eco*-ADH) were optimized and synthesized following BamHI and XhoI restriction digestion and cloning into the pET28a(+) vector. Both ligation constructs were used to transform *E. coli* C41 cells. Seed culture (1 mL seed) was added to 100 mL of LB medium containing kanamycin (100 μg/mL) and grown at 37 °C and 200 rpm. The cells were induced with isopropyl β-D-1-thiogalactopyranoside (0.5 mM) for overexpression after they reached an optical density of 0.6 at 600 nm; then, they were incubated at 25 °C for 16 h for protein synthesis. The cells were harvested by ultracentrifugation at 3500 rpm for 20 min, and dry cells were washed twice with washing buffer (50 mM potassium phosphate buffer), followed by lysis *via* sonication. The lysate was then centrifuged at 10,000 rpm for 10 min, and the supernatant was mixed with resin for purification. The resin-bound proteins were eluted with different concentrations of

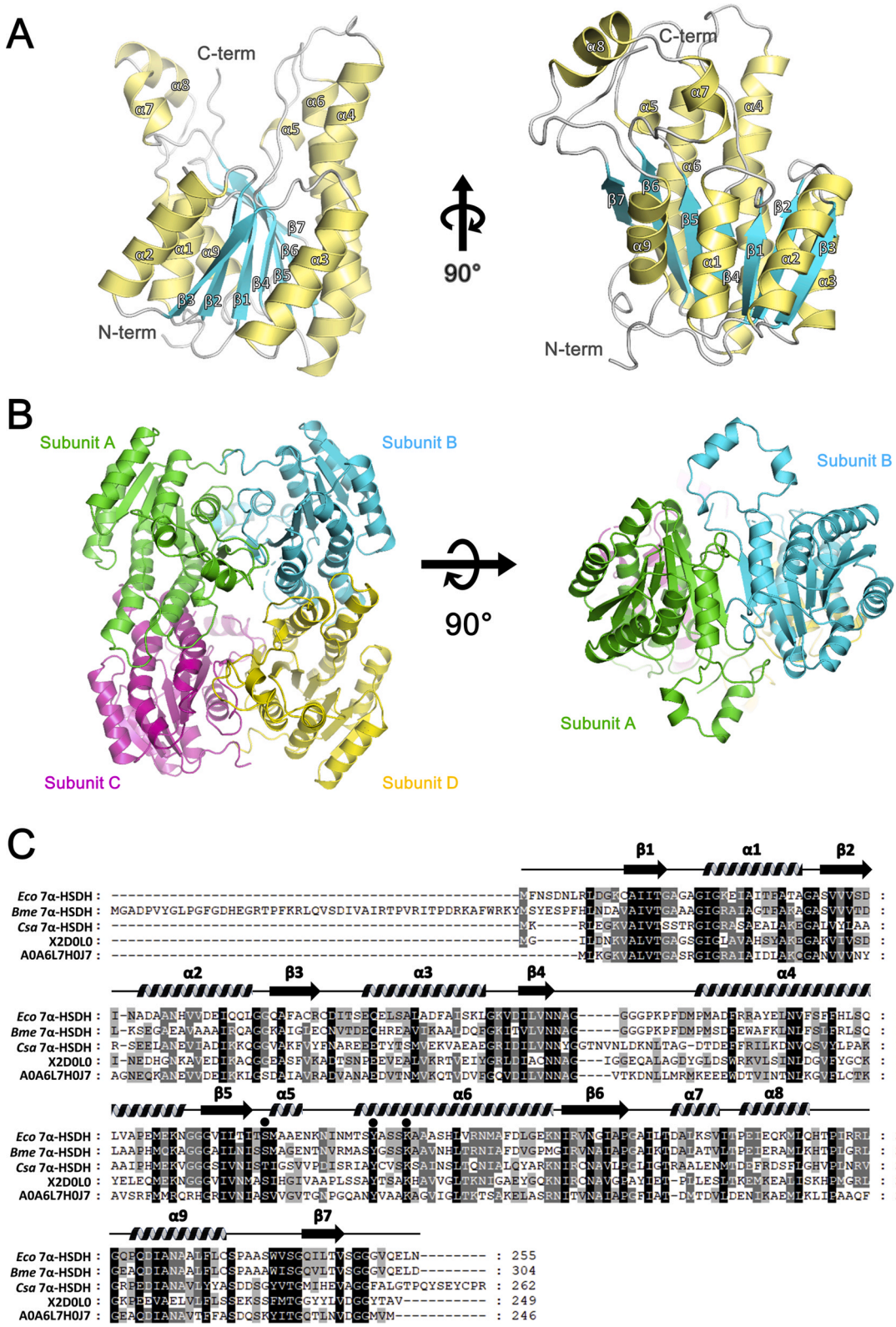

Fig. 1. Crystal structure of apo *Eco*-7α-HSDH. (A) Overall monomer structure of *Eco*-7α-HSDH (chain A) is shown in front and 90°-rotated views. Ribbon representation of *Eco*-7α-HSDH (chain A) with the β-strands in cyan and α-helices in yellow. (B) Tetramer structure of *Eco*-7α-HSDH. (C) Multiple sequence alignment of *Eco*-7α-HSDH with homologous proteins. Aligned sequences include *Eco*-7α-HSDH (UniProtKB: P0AET8), *Bme*-7α-HSDH (UniProtKB: Q8YIN7), *Cab*-7α-HSDH (UniProtKB: G9FRD7), short-chain dehydrogenase reductase from *Chryseobacterium* sp. (UniProtKB: X2D0L0), and 3-oxoacyl-ACP reductase from *Bacillus anthracis* (UniProtKB: A0A6L7H0J7). The catalytically important residues (S146, Y159, and K163) are indicated with black circles.
Bme-7α-HSDH, *Brucella melitensis* 7α-HSDH; *Cab*-7α-HSDH, *Clostridium absonum* 7α-hydroxysteroid dehydrogenase; *Eco*-7α-HSDH, *Escherichia coli* 7α-hydroxysteroid dehydrogenase.

Table 2
Structural homolog search results for *Eco*-7α-HSDH (DALI-Lite server).

Protein name	PDB code	DALI Z-score	UniProtKB code	Ligand	Reference
Eco-7α-HSDH	1AHH	43.3	P0AET8	NAD^+	[5]
Eco-7α-HSDH	1AHI	41.8	P0AET8	NADH, 7-oxoglycochenodeoxycholic acid	[5]
Bme-7α-HSDH	3GAF	41.7	Q8YIN7	No	Unpublished
Ketone reductase ChKRED20 from *Chryseobacterium* sp. CA49	5 × 8H	36.0	X2D0L0	No	(2017) Appl Microbiol Biotechnol 101: 8395−8404
3-oxoacyl-ACP reductase from *Bacillus anthracis*	2UVD	35.9	A0A6L7H0J7	No	(2008) Proteins 70: 562−567
NADH-dependent FabG from *Cupriavidus taiwanensis*	4NBV	35.8	B3R6T4	Bis-tris propane	(2014) Appl Environ Microbiol 80: 497−505
Cyclohexanol dehydrogenase from *Aromatoleum aromaticum*	4URF	35.7	Q5P8S7	NAD^+,	(2015) J Mol Microbiol Biotechnol 25: 327−339

Bme-7α-HSDH, *Brucella melitensis* 7α-hydroxysteroid dehydrogenase; *Eco*-7α-HSDH, *Escherichia coli* 7α-hydroxysteroid dehydrogenase; PDB, Protein Data Bank.

imidazole and concentrated using a 30-kDa filter for *Eco*-ADH and 10-kD filter for *Eco*-7α-HSDH (Centricon; Millipore, Billerica, MA, USA).

2.3. Co-factor regeneration system

Because *Eco*-7α-HSDH requires NAD^+ as a co-factor for catalysis, we used ADH with the co-substrate acetone for efficient NAD^+ regeneration (Scheme 1). The efficiency of 7-KLCA production from CDCA was observed with different concentrations of *Eco*-ADH. The *in vitro* reaction was conducted using 7α-HSDH (2 mg/mL), CDCA (10 mM), DTT (1 mM), ADH (4 mg/mL), NAD^+ (0.5 mM), and 10 % acetone in 500 μL of potassium phosphate buffer (pH 7.4) for 1 h. The reaction mixture was extracted with double volume ethyl acetate, and then dried with nitrogen gas and was dissolved in methanol for analysis.

We cloned *Eco*-ADH into the pET32a(+) vector and used it to transform C41 cells harboring the *Eco*-7α-HSDH pET28a(+) plasmid for *in vivo* biotransformation. Cells were overexpressed, and dry cells were obtained as described above. These cells were then suspended in potassium phosphate buffer, and *the in vivo* biotransformation of CDCA to 7-KLCA was performed in a 1-mL reaction (1.0 g/mL cell dry weight) containing CDCA (10 mM) and 10 % acetone in a 500-μL reaction volume of potassium phosphate buffer (pH 7.4) for 2 h.

2.4. Analytical methods

The substrate and product were analyzed using an evaporation light-scattering detector (ELSD) (ESA6700; Chromaflo Technologies, Ashtabula, OH, USA), and the samples were separated using a Mightysil reverse-phase C18 GP column (4.6 mm × 250 mm, 5 μm; Kanto Chemical, Tokyo, Japan). The reaction mixture was eluted using a gradient system of water (A) and acetonitrile (B). Pump B concentration was gradually increased from 10 % to 100 % for 27 min and gradually decreased to 10 % for 35 min at a flow rate of 1.5 mL/min. The sample mixture was nebulized at 60 °C and 350 kPa pressure (nitrogen gas). The reaction mixtures were analyzed by SYNAPT G2-S/ACUITY UPLC liquid-chromatography (LC) quadrupole time-of-flight/electrospray ionization mass spectrometry (MS; water) in the positive ion mode.

2.5. Crystallization and data collection

Crystallization screening of *Eco*-7α-HSDH was performed in 96-well crystallization plates (Emerald Bio, Bainbridge Island, WA, USA) at 293 K using the sitting-drop vapor-diffusion method. A high-throughput Mosquito crystallization robot (SPT Labtech, Basingstoke, UK) was used with several commercially available crystallization screening kits [MCSG I-IV (Anatrace, Maumee, OH, USA), Index, and SaltRx (Hampton Research Aliso Viejo, CA, USA)]. Drops consisting of 200 nL of protein solution and 200 nL of reservoir solution were equilibrated against 80 μL of reservoir solution. Crystals were grown in the presence of 0.1 M HEPES:NaOH pH 7.5, 20 % (w/v) PEG 4000, and 10 % (v/v) 2-propanol (MCSG4 #G11), and after 2 days of incubation at 293 K, single crystals were harvested and mounted without cryoprotectant. X-Ray diffraction data were collected on a BL-5C beamline at the Pohang Accelerator Laboratory (Pohang, Korea). The dataset containing 180 images with 1° rotation was indexed, integrated, and scaled using the *HKL-2000* program [18].

2.6. Structure determination and refinement

The crystal structure of *Eco*-7α-HSDH was determined at 2.7 Å resolution by molecular replacement using *MOLREP* from the *CCP4i* suite [19,20] and with NADH-bound *Eco*-7α-HSDH (PDB: 1FMC) as a template model [5]. Iterative model rebuilding and refinement were performed using *COOT* [21], *REFMAC5* [22], and *phenix.refine* [23]. The final structure model of *Eco*-7α-HSDH checked using *MolProbity* [24] had R_{work} and R_{free} values of 0.195 and 0.276, respectively. The detailed X-ray data collection and refinement statistics are presented in Table 1. The coordinate and structural factors for *Eco*-7α-HSDH have been deposited in the Protein Data Bank (http://www.rcsb.org/; accession code: 7ENY). Structural figures were generated using the PyMOL program [25].

3. Results and discussion

3.1. Apo structure of Eco-7α-HSDH

To investigate the structural changes associated with substrate and co-factor binding, we determined the apo structure of *Eco*-7α-HSDH at 2.7 Å resolution. The *Eco*-7α-HSDH crystals belonged to space group $P2_1$, with two tetrameric molecules in the asymmetric unit. The structure was solved by molecular replacement using the monomer *Eco*-7α-HSDH structure (NAD^+-complexed structure; PDB: 1AHH) [5] following the removal of NAD and water molecules. Data collection and refinement statistics are summarized in Table 1.

The overall structure of apo *Eco*-7α-HSDH has Rossmann-fold motifs with nine α-helices and seven β-strands (Fig. 1A) and shows a homotetrameric quaternary structure, which was in accordance with previous analysis of the oligomeric state of this same enzyme and our size-exclusion chromatography results (Fig. 1B). Interestingly, the four chains in the functional tetramer displayed significant conformational differences in the β4-α4 loop, α7-α8 helices, and C-terminal loop, as illustrated by the superposition of the four-subunit structures (Fig. 1C). This is discussed in detail in the following section.

Searches for structural homologs using the DALI server [26] revealed that apo *Eco*-7α-HSDH showed a high degree of structural similarity with binary- and ternary-complexed *Eco*-7α-HSDH structures. Additionally, the DALI search showed that apo *Eco*-7α-HSDH shares remarkable similarity with *Bme*-7α-HSDH (PDB: 3GAF; DALI z-score: 41.7), ketone reductase ChKRED20 from *Chryseobacterium* sp. CA49 (PDB: 5 × 8H; DALI z-score: 36.0), 3-oxoacyl-ACP reductase from *B. anthracis* (PDB:

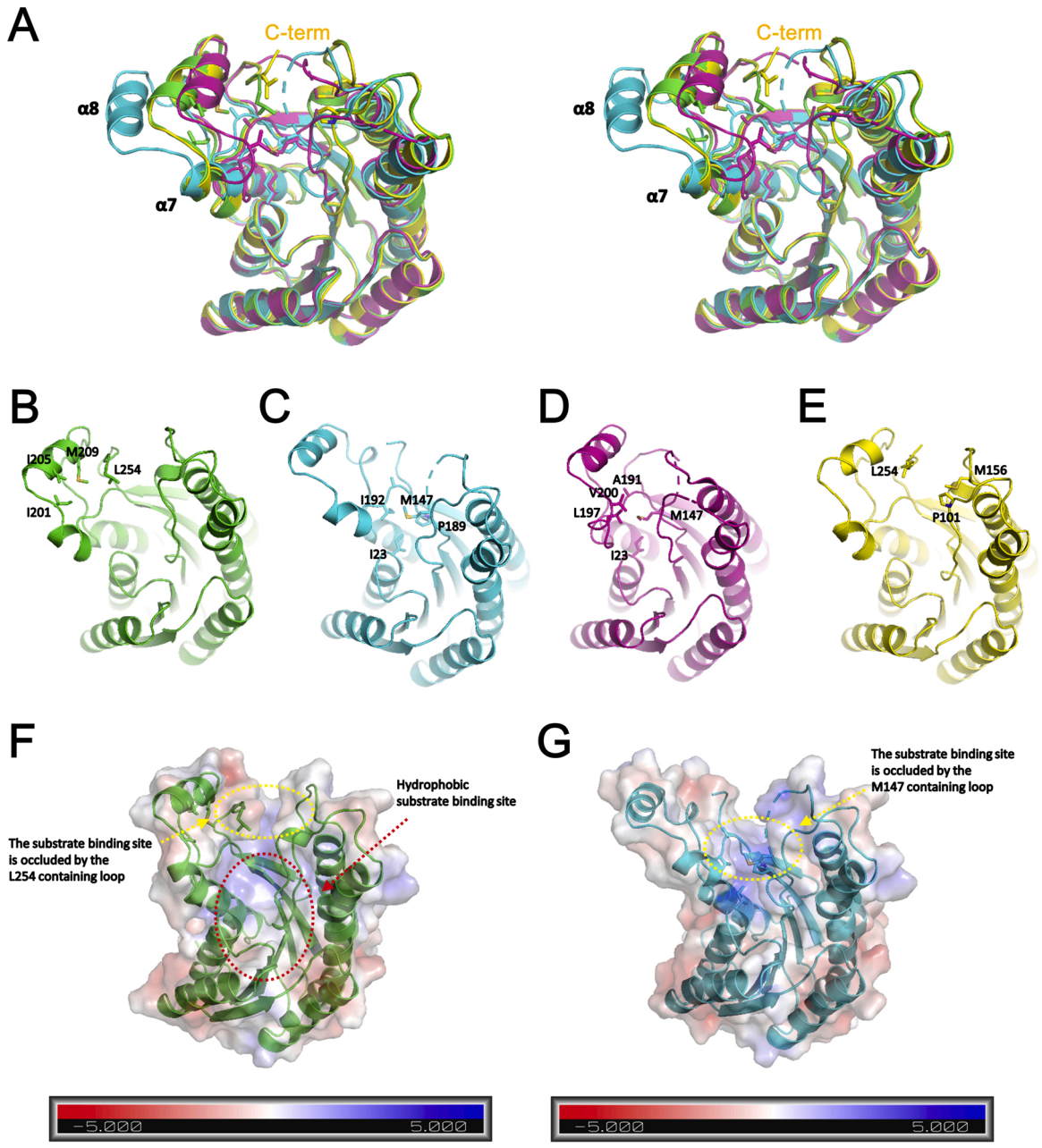

Fig. 2. Structural comparison of four subunits in apo *Eco*-7α-HSDH. (A) Superposition of the four subunits (chains A–D; colors identical to those identified in Fig. 1B) in stereoview. Cartoon representations of (B) chain A and (E) chain D, where residue L254 blocks the entrance to the substrate-binding site. Cartoon representations of (C) chain B and (D) chain C, where residue M147 blocks the entrance to the substrate-binding site. Electrostatic charge surface view of (F) chain A and (G) chain B. *Eco*-7α-HSDH, *Escherichia coli* 7α-hydroxysteroid dehydrogenase.

2UVD; DALI z-score: 35.9), NADH-dependent FabG from *Cupriavidus taiwanensis* (PDB: 4NBV; DALI z-score: 35.8), and cyclohexanol dehydrogenase from *Aromatoleum aromaticum* (PDB: 4URF; DALI z-score: 35.7) (Table 2).

3.1.1. Apo Eco-7α-HSDH has intrinsic structural flexibility in the β4-α4 loop and C-terminal loop regions and the α7-α8 helices

The structural superposition results obtained using four subunits in the apo *Eco*-7α-HSDH structure showed that significant conformational changes appeared in three regions: the β4-α4 loop, α7-α8 helices, and C-terminal loop (Fig. 2A). The α7-α8 helices form the most open conformation in the chain B structure (Fig. 2B–E). Notably, the α7-α8 helix region formed crystal-packing interactions with the neighboring molecules (Figure S1). Additionally, the chain C structure has a closed conformation, where the α7-helix is partially unfolded. Moreover, the β4-α4 loop includes missing and non-modeled residues (148–151) in chain B and (149–152) chain C, indicating that this region has a high degree of flexibility. The co-factor-binding site is located at one end of the β-sheet, and the substrate-binding site is located at the upper position of the co-factor-binding site. Furthermore, the electrostatic surface-charge distribution showed that the substrate-binding site is hydrophobic. In the apo *Eco*-7α-HSDH structure, the substrate-binding site was capped and covered by the β4-α4 loop or C-terminal loop, both of which bend over the active site and block the hydrophobic substrate-binding site. The C-terminal region covered the substrate-binding site in the chain A and chain D structures, and the L254 residue in the C-terminal loop forms hydrophobic interactions with the α5-α6 and α8-helix regions (Fig. 2F). In contrast, the β4-α4 loop covers the hydrophobic substrate-

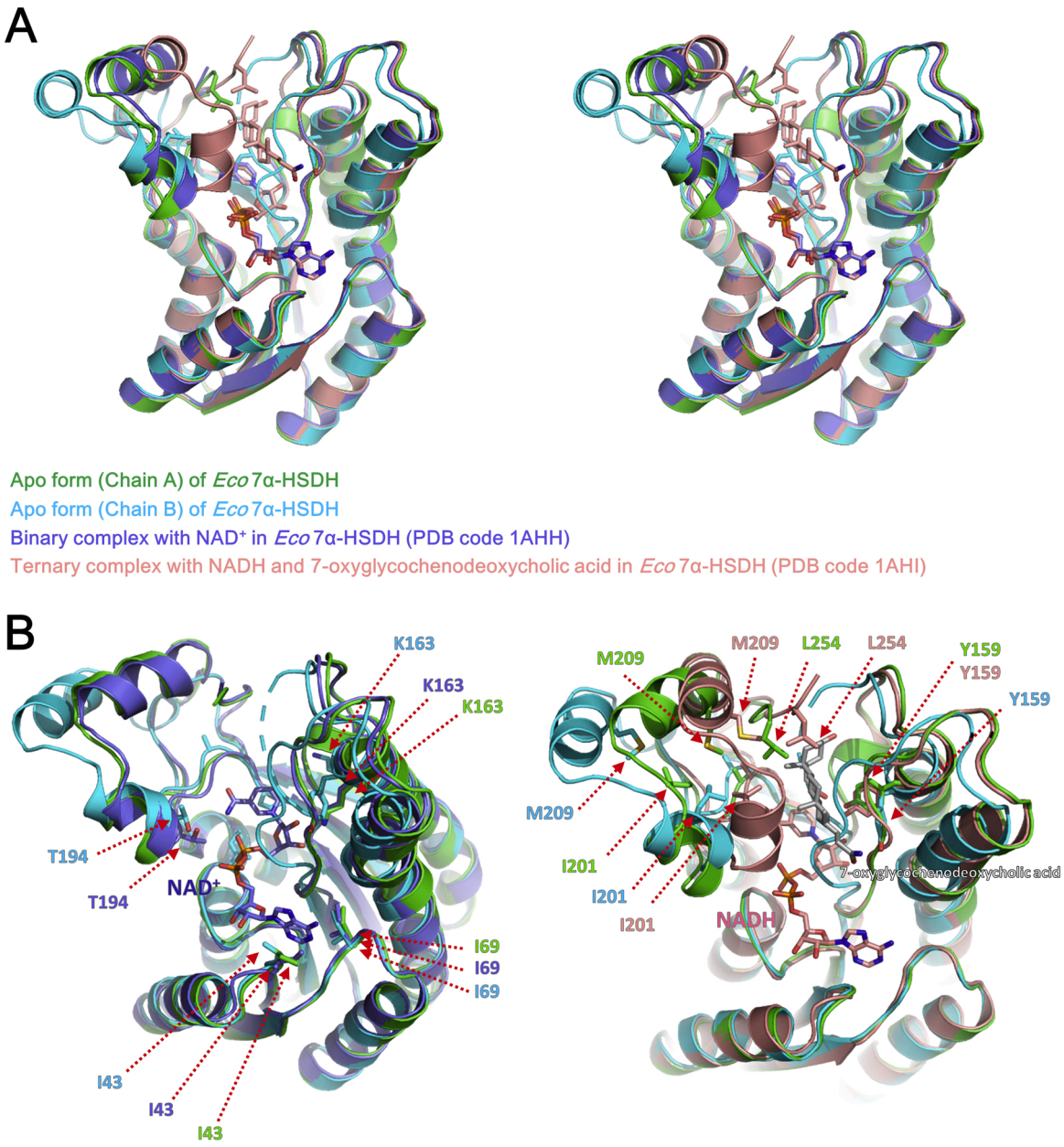

Fig. 3. Structural comparison of apo *Eco*-7α-HSDH with the binary- and ternary-complex structures. (A) Stereoview of the structural superposition of apo *Eco*-7α-HSDH (chains A and B) with the binary (PDB: 1AHH)- and ternary (PDB: 1AHI)-complex structures. Residues undergoing structural changes by (B) NAD^+ binding and (C) 7-oxoglycochenodeoxycholic acid binding are indicated by stick models.
Eco-7α-HSDH, *Escherichia coli* 7α-hydroxysteroid dehydrogenase.

binding site in the chain B and chain C structures. In particular, the M147 residue located on the β4-α4 loop makes hydrophobic interactions with residues in the β6-α8 loop and α7-helix regions (Fig. 2G), which result in the extrusion of the β4-α4 loop into the substrate-binding pocket. These findings revealed that the apo *Eco*-7α-HSDH structure has an open conformation due to α7-α8 helix movement, although the substrate-binding site is blocked by the β4-α4 loop or C-terminal loop. We speculated that blocking substrate binding might prohibit nonspecific hydrophobic molecules from entering the substrate-binding site of apo *Eco*-7α-HSDH.

3.1.2. Structural comparison of apo Eco-7α-HSDH with the binary- and ternary-complex structures

A structural comparison of the apo structure with the binary (PDB: 1AHH) and ternary-complex (PDB: 1AHI) [5] structures of *Eco*-7α-HSDH revealed that the conformation of the α7-α8 helices represented the primary difference between the three structures (Fig. 3A). The structure of the ternary complex has a fully closed conformation due to the closing movement of the α7-α8 helices. Chain B of the apo structure showed the widest open conformation, whereas chain A resembled the co-factor-bound binary-complex structure, although there was a slight closing movement by the α7-α8 helices and conformational changes in the I43, I69, and R194 side chains promoting interaction with NAD^+. Additionally, K163 in chain B of the apo structure showed substantial structural movement relative to that observed in chain A of both apo and binary-complex structures (Fig. 3B). These findings suggest that the binary-complex structure of *Eco*-7α-HSDH showed a semi-closed conformation, whereas only the ternary-complex structure has a fully closed structure. In contrast, the apo *Eco*-7α-HSDH subunits demonstrate a consistently open conformation, although the degree of opening differs

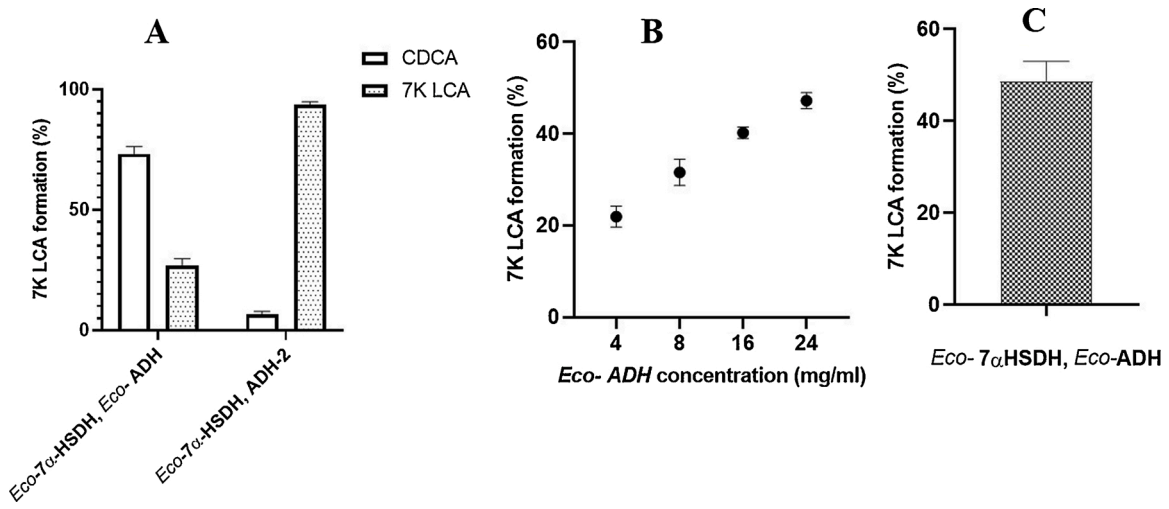

Fig. 4. Product (7-KLCA) formation using different combinatorial approaches. (A) The reaction included *Eco*-7α HSDH (2 mg/mL), *Eco*-ADH/ADH-2 (2 mg/mL), CDCA (10 mM), DTT (1 mM), NAD^+ (0.5 mM), and 10 % acetone in 500 μL of potassium phosphate buffer (pH 7.4); the reaction was performed for 1 h. (B) *In vitro* 7-KLCA formation along with increasing Eco-ADH concentration. (C) *In vivo* 7-KLCA formation using the co-substrate acetone in the presence of *Eco*-ADH for NAD^+ regeneration.

7-KLCA, 7-ketolithocholic acid; ADH, alcohol dehydrogenase; CDCA, chenodeoxycholic acid; *Eco*-7α-HSDH, *Escherichia coli* 7α-hydroxysteroid dehydrogenase; *Eco*-ADH, *Escherichia coli* alcohol dehydrogenase.

from the other structure due to intrinsic structural flexibility. Structural comparisons of the open and fully closed conformations indicated that the Y159, L254, M209, and I201 residues undergo a large conformational change upon substrate binding. A previous study proposed that S146, Y159, and K163 are important for the catalytic process of *Eco*-7α-HSDH. Specifically, Y159 might act as a catalytic residue, whereas S146 and K163 play important roles in substrate and co-factor binding, respectively (Fig. 3C).

The structure information of apo *Eco*-7α-HSDH enabled us to evaluate serial structural changes by prior co-factor (NAD^+) binding, followed by substrate binding. Moreover, four chain structures in apo *Eco*-7α-HSDH have different conformations in the β4-α4 loop, β5-α6 loop, α7-α8 helices, and C-terminal loop regions. This enabled us to examine conformation and interaction changes during initial co-factor binding. The co-factor binding induced the movement of the β4-α4 (residues 95–107) and β5-α6 loops (residues 145–155) in *Eco*-7α-HSDH. In the apo chain B and C structures, these two loops are extruded to the center of the co-factor-binding site. However, the two loops move back and form tight interactions with the bound co-factor. Structural superposition of the apo structure (chains B and C) and binary complex (PDB code 1AHH) showed that the Met147 residue is located in the corresponding position of the nicotinamide group of bound NAD. Another notable conformation change is the flip motion of the side chain of Tyr159. The Tyr159 residue of the apo structure (chains B and C) is located in the β4-α4 loop of binary complex structure. After co-factor binding, the side chain of Tyr159 is flipped to the inner side of the co-factor-binding pocket and directed to the ribose sugar ring of bound co-factor (Figure S2A). The following substrate binding might be related to the closing movement of the α7-α8 helices (residues 195–211) and conformational changes in the C-terminal loop region (residues 247–255). It should be noted that the Met209 and Leu254 residues are directly involved in substrate binding by forming hydrophobic interactions. In the ternary complex structure (PDB code 1AHI), the bound substrate (7-oxoglycochenodeoxycholic acid) forms hydrophobic interactions with the co-factor (NADH) and the Tyr159 residue (Figure S2B). Thus, it is thought that co-factor binding may facilitate and induce substrate binding.

3.2. Biotransformation of CDCA to 7-KLCA using a co-factor-regeneration system

Following successful co-expression and purification of *Eco*-7α-HSDH and *Eco*-ADH (Figure S3), we observed efficient catalysis of CDCA to 7-KLCA using the ADH system for co-factor recycling. The retention time was 22.4 min for the product (7-KLCA), which existed as a dimer with a mass of 781.564 *m/z* according to the LC–MS analysis (Figure S4). *Eco*-7α-HSDH catalysis requires the co-factor NAD^+ [5], which is expensive. Prabha et al. [7] reported *Eco*-7α-HSDH activity in the presence of CDCA and other C-7 hydroxyl bile acids, demonstrating increased enzyme activity in the presence of ions and chelating agents. Additionally, Huang et al. [27] demonstrated upregulated 7-KLCA production by $NADP^+$-dependent 7α-HSDH from *C. absonum* using D-amino acid dehydrogenase for $NADP^+$ regeneration. In the present study, we introduced the *Eco*-ADH system for NAD^+ recycling, which can then be used by *Eco*-7α-HSDH for catalysis (Scheme 1 and Fig. 4). We found that increased *Eco*-ADH concentration along with constant levels of *Eco*-7α-HSDH, NAD^+, and substrate doubled the production of 7-KLCA in the *in vitro* reaction (Fig. 4B). A comparison of the *Eco*-7α-HSDH activity using commercial ADH-2 with that using *Eco*-ADH under similar optimum conditions revealed that the NAD^+-regeneration system using ADH-2 showed >95 % conversion of CDCA to 7-KLCA (Fig. 4A). Moreover, *Eco*-7α-HSDH and *Eco*-ADH in the *in vivo* system resulted in ~50 % product formation (Fig. 4C). It is possible that optimization and use of ADH might be a crucial first step in co-factor regeneration during UDCA production from CDCA. Similarly, a previous study used lactate dehydrogenase with pyruvate as a co-substrate for NAD^+ recycling with *Eco*-7α-HSDH to synthesize a 7-KLCA intermediate during the two-step synthesis of UDCA (Zheng et al., 2015). Large-scale production of UDCA from CDCA has been achieved using 7α-HSDH from *C. absonum* and 7β-HSDH from *Ruminococcus torques* and a sufficient amount of $NADP^+$ co-factors [28]. In the present study, we demonstrated efficient and reliable synthesis of a 7-KLCA intermediate using *Eco*-7α-HSDH in the presence of *Eco*-ADH for co-factor regeneration targeting UCDA synthesis.

In conclusion, we solved the structure of apo *Eco*-7α-HSDH, which allowed elucidation of conformational changes in three key structural elements (the β4-α4 loop, α7-α8 helices, and C-terminal loop) associated with co-factor and substrate binding. These structural alterations

reposition catalytically important residues and enable catalysis. Additionally, we observed that L254 and M147 act as gatekeepers to block the substrate-binding site in apo *Eco*-7α-HSDH before co-factor and substrate binding. Furthermore, we developed an efficient method to assess *Eco*-7α-HSDH activity through co-expression with *Eco*-ADH, which enables co-factor recycling through 7-KLCA generation from CDCA *via Eco*-7α-HSDH.

Funding

This research was a part of the project titled "Development of potential antibiotic compounds using polar organism resources" (15250103, KOPRI Grant PM21030) funded by the Ministry of Oceans and Fisheries, Korea.

Declaration of Competing Interest

None.

Acknowledgments

We thank the staff at the X-ray core facility of the Korea Basic Science Institute (Ochang, Korea) and BL-5C of the Pohang Accelerator Laboratory (Pohang, Korea) for their assistance with data collection.

Appendix A. Supplementary data

Supplementary material related to this article can be found, in the online version, at doi:https://doi.org/10.1016/j.jsbmb.2021.105945.

References

[1] V. Prabha, M. Ohri, Bacterial transformations of bile acids, World J. Microbiol. Biotechnol. 22 (2006) 191–196.
[2] J.A. Sherrod, P.B. Hylemon, Partial purification and characterization of NAD-dependent 7alpha-hydroxysteroid dehydrogenase from *Bacteroides thetaiotaomicron*, Biochim. Biophys. Acta 486 (1977) 351–358, https://doi.org/10.1016/0005-2760(77)90031-5.
[3] G. Ottolina, S. Riva, G. Carrea, B. Danieli, A.F. Buckmann, Enzymatic synthesis of [4R-2H]NAD (P)H and [4S-2H]NAD(P)H and determination of the stereospecificity of 7 alpha- and 12 alpha hydroxysteroid dehydrogenase, Biochim. Biophys. Acta 998 (1989) 173–178, https://doi.org/10.1016/0167-4838(89)90270-7.
[4] P. Lepercq, P. Gerard, F. Beguet, P. Raibaud, J.P. Grill, P. Relano, C. Cayuela, C. Juste, Epimerization of chenodeoxycholic acid to ursodeoxycholic acid by *Clostridium baratii* isolated from human feces, FEMS Microbiol. Lett. 235 (2004) 65–72.
[5] N. Tanaka, T. Nonaka, T. Tanabe, T. Yoshimoto, D. Tsuru, Y. Mitsui, Crystal structures of the binary and ternary complexes of 7alpha-hydroxysteroid dehydrogenase from *Escherichia coli*, Biochemistry 35 (1996) 7715–7730, https://doi.org/10.1021/bi951904d.
[6] T. Tanabe, N. Tanaka, K. Uchikawa, T. Kabashima, K. Ito, T. Nonaka, Y. Mitsui, M. Tsuru, T. Yoshimoto, Roles of the Ser146, Tyr159, and Lys163 residues in the catalytic action of 7alpha-hydroxysteroid dehydrogenase from *Escherichia coli*, J. Biochem. 124 (1998) 634–641, https://doi.org/10.1093/oxfordjournals.jbchem.a022159.
[7] V. Prabha, M. Gupta, K.G. Gupta, Kinetic properties of 7α-hydroxysteroid dehydrogenase from *Escherichia coli* 080, Can. J. Microbiol. 35 (1989) 1076–1080, https://doi.org/10.1139/m89-180.
[8] M.J. Bennett, S.L. McKnight, J.P. Coleman, Cloning and characterization of the NAD-dependent 7-alpha-hydroxysteroid dehydrogenase from Bacteroides fragilis, Curr. Microbiol. 47 (2003) 475–484, https://doi.org/10.1007/s00284-003-4079-4.
[9] D. Zhu, J.E. Stearns, M. Ramirez, L. Hua, Enzymatic enantioselective reduction of α-ketoesters by a thermostable 7α-hydroxysteroid dehydrogenase from Bacteroides fragilis, Tetrahedron 62 (2006) 4535–4539.
[10] A. Medici, P. Pedrini, E. Bianchini, G. Fantin, A. Guerrini, B. Natalini, R. Pellicciari, 7α-OH epimerisation of bile acids via oxido-reduction with *Xanthomonas maltophilia*, Steroids 67 (2002) 51–56.
[11] J.P. Coleman, L.L. Hudson, M.J. Adams, Characterization and regulation of the NADP-linked 7 alpha-hydroxysteroid dehydrogenase gene from *Clostridium sordellii*, J. Bacteriol. 176 (1994) 4865–4874.
[12] D. Bakonyi, W. Hummel, Cloning, expression, and biochemical characterization of a novel NADP+-dependent 7α-hydroxysteroid dehydrogenase from *Clostridium difficile* and its application for the oxidation of bile acids, Enzyme Microb. Technol. 99 (2017) 16–24.
[13] E.E. Ferrandi, G.M. Bertolesi, F. Polentini, A. Negri, S. Riva, D. Monti, In search of sustainable chemical processes: cloning, recombinant expression, and functional characterization of the 7α- and 7β-hydroxysteroid dehydrogenases from *Clostridium absonum*, Appl. Microbiol. Biotechnol. 95 (2012) 1221–1233, https://doi.org/10.1007/s00253-011-3798-x.
[14] D. Lou, B. Wang, J. Tan, L. Zhu, X. Cen, Q. Ji, Y. Wang, The three-dimensional structure of *Clostridium absonum* 7α-hydroxysteroid dehydrogenase: new insights into the conserved arginines for NADP (H) recognition, Sci. Rep. 6 (2016) 1–11.
[15] D. Lou, Y. Wang, J. Tan, L. Zhu, S. Ji, B. Wang, Functional contribution of coenzyme specificity-determining sites of 7α-hydroxysteroid dehydrogenase from *Clostridium absonum*, Comput. Biol. Chem. 70 (2017) 89–95.
[16] F. Tonin, I.W.C.E. Arends, Latest development in the synthesis of ursodeoxycholic acid (UDCA): a critical review, Beilstein J. Org. Chem. 14 (2018) 470–483, https://doi.org/10.3762/bjoc.14.33.
[17] D. Monti, G. Ottolina, G. Carrea, S. Riva, Redox reactions catalyzed by isolated enzymes, Chem. Rev. 111 (2011) 4111–4140.
[18] Z. Otwinowski, W.I. Minor, Processing of X-ray diffraction data collected in oscillation mode, in: C.W. Carter Jr., R.M. Sweet (Eds.), Methods in Enzymology, Vol. 276: Macromolecular Crystallography, Part A, Academic Press, Cambridge, 1997, pp. 307–326.
[19] A. Vagin, A. Teplyakov, Molecular replacement with MOLREP, Acta Crystallogr. D Biol. Crystallogr. 66 (2010) 22–25.
[20] M.D. Winn, C.C. Ballard, K.D. Cowtan, E.J. Dodson, P. Emsley, P.R. Evans, R. M. Keegan, E.B. Krissinel, A.G.W. Leslie, A. McCoy, S.J. McNicholas, G. N. Murshudov, N.S. Pannu, E.A. Potterton, H.R. Powell, R.J. Read, A. Vagin, K. S. Wilson, Overview of the CCP4 suite and current developments, Acta Crystallogr. D Biol. Crystallogr. 67 (2011) 235–242.
[21] P. Emsley, K. Cowtan, Coot: model-building tools for molecular graphics, Acta Crystallogr, D Biol. Crystallogr. 60 (2004) 2126–2132.
[22] G.N. Murshudov, P. Skubak, A.A. Lebedev, N.S. Pannu, R.A. Steiner, R.A. Nicholls, M.D. Winn, F. Long, A.A. Vagin, REFMAC5 for the refinement of macromolecular crystal structures, Acta Crystallogr. D Biol. Crystallogr. 67 (2011) 355–367.
[23] P.V. Afonine, R.W. Grosse-Kunstleve, N. Echols, J.J. Headd, N.W. Moriarty, M. Mustyakimov, T.C. Terwilliger, A. Urzhumtsev, P.H. Zwart, P.D. Adams, Towards automated crystallographic structure refinement with phenix. Refine, Acta Crystallogr. D Biol. Crystallogr. 68 (2012) 352–367.
[24] V.B. Chen, W.B. Arendall, J.J. Headd, D.A. Keedy, R.M. Immormino, G.J. Kapral, L. W. Murray, J.S. Richardson, D.C. Richardson, MolProbity: all-atom structure validation for macromolecular crystallography, Acta Crystallogr, D Biol. Crystallogr. 66 (2010) 12–21.
[25] W.L. DeLano, The PyMOL Molecular Graphics System, DeLano Scientific, San Carlos, CA, USA, 2002.
[26] L. Holm, Benchmarking fold detection by DaliLite v. 5, Bioinformatics 35 (2019) 5326–5327.
[27] B. Huang, Q. Zhao, J.H. Zhou, G. Xu, Enhanced activity and substrate tolerance of 7α-hydroxysteroid dehydrogenase by directed evolution for 7-ketolithocholic acid production, Appl. Microbiol. Biotechnol. 103 (2019) 2665–2674, https://doi.org/10.1007/s00253-019-09668-4.
[28] X. Zhang, D. Fan, X. Hua, T. Zhang, Large-scale production of ursodeoxycholic acid from chenodeoxycholic acid by engineering 7A- and 7B-hydroxysteroid dehydrogenase, Bioprocess Biosyst. Eng. 42 (2019) 1537–1545, https://doi.org/10.1007/s00449-019-02151-4.